Title

A bench-top model of middle ear effusion diagnosed with optical tympanometry

Authors

Shreim, Samir

Abouzari, Mehdi

Weidling, John

et al.

Publication Date

2020-07-01

DOI

10.1016/j.ijporl.2020.110054

Peer reviewed

HHS Public Access

Author manuscript

Int J Pediatr Otorhinolaryngol. Author manuscript; available in PMC 2021 July 01.

Published in final edited form as:

Int J Pediatr Otorhinolaryngol. 2020 July ; 134: 110054. doi:10.1016/j.ijporl.2020.110054.

A Bench-Top Model of Middle Ear Effusion Diagnosed with Optical Tympanometry

Samir Shreim, PhD[1,*], **Mehdi Abouzari, MD, PhD**[2,3,*], **John Weidling, PhD**[1], **Sean White, PhD**[1], **Khodayar Goshtasbi, BS**[2], **Nguyen Pham, MD**[2,3], **Hamid R. Djalilian, MD**[2,4], **Elliot Botvinick, PhD**[1,4]

[1]Beckman Laser Institute, University of California, Irvine, USA

[2]Department of Otolaryngology–Head and Neck Surgery, University of California, Irvine, USA

[3]Division of Pediatric Otolaryngology, Children's Hospital of Orange County, Orange, USA

[4]Department of Biomedical Engineering, University of California, Irvine, USA

Abstract

Objectives: To assess the validity of a bench-top model of an optical tympanometry device to diagnose *in vitro* model of middle ear effusion (MEE).

Methods and Materials: We illuminated an *in vitro* model of ear canal and tympanic membrane with broadband light and relayed remitted light to a spectrometer system. We then used our proprietary algorithm to extract spectral features that, together with our logistic regression classifiers, led us to calculate a set of simplified indices related to different middle ear states. Our model included a glass vial covered with a porcine submucosa (representing the tympanic membrane) and filled with air, water, or milk solution (representing different MEE), and a set of cover-glass slips filled with either blood (representing erythema) or cerumen. By interchanging fluid types and cover-glass slips, we made measurements on combinations corresponding to normal healthy ear and purulent or serous MEE.

Results: Each simulated condition had a distinct spectral profile, which was then employed by our algorithm to discriminate clean and cerumen-covered purulent and serous MEE. Two logistic purulent and serous MEE classifiers correctly classified all *in vitro* middle ear states with 100% accuracy assessed by leave-one-out and k-fold cross validation.

Conclusions: This proof-of-concept *in vitro* study addressed an unmet need by introducing a device that easily and accurately can assess middle ear effusion. Future *in vivo* studies aimed at

Corresponding authors: Hamid R. Djalilian, MD, Division of Neurotology and Skull Base Surgery, Department of Otolaryngology–Head and Neck Surgery, University of California Irvine, 19182 Jamboree Road, Otolaryngology-5386, Irvine, CA 92697, Phone: (714) 456-5753, Fax: (714) 456-5747, hdjalili@hs.uci.edu, Elliot Botvinick, PhD, Beckman Laser Institute, University of California Irvine, 1002 Health Sciences Road, Irvine, CA, 92612, Phone: (949) 824-9613, Fax: (949) 824-8413, elliot.botvinick@uci.edu.
*These authors contributed equally to this manuscript.

Conflicts of Interest: None

collecting data from clinical settings are warranted to further elucidate the validity of the technology in diagnosing pediatric acute otitis media.

Keywords

otitis media; middle ear effusion; optical tympanometry; diagnostic device; children; *in vitro* model

1. Introduction

Otitis media (OM) is one of the most common childhood conditions resulting in nearly 30 million office and emergency room visits annually in the U.S., with a roughly $5 billion healthcare cost.[1–5] It is also the leading cause of unnecessary antibiotic use in children, causing undesirable risk for side effects and resistance.[6] Diagnosis of OM can be challenging for two reasons. Children affected by OM are most often too young to adequately describe their symptoms. Additionally, though OM signs are numerous, they can be very non-specific.[7] Clinical diagnosis is most commonly done using an otoscope to assess the presence of a middle ear inflammation and fluid. Unfortunately, visualization is frequently (~50% of cases) limited by cerumen within the small ear canals of children.[7] Furthermore, a crying child can result in erythema and sometimes bulging of the tympanic membrane unrelated to OM, making erythema alone not sensitive for the diagnosis of OM.

The difficulty of achieving accurate OM diagnosis within the limits of currently available technology is well recognized. In their most recent clinical practice guidelines, the American Academy of Otolaryngology-Head and Neck Surgery Foundation (AAO-HNSF) and the American Academy of Pediatrics (AAP) specifically request new technology, stating “devices that more accurately identify the presence of middle ear effusion and ear drum bulging that are easier to use than tympanometry during office visits would be welcome, especially in the difficult-to-examine infant”.[5,8] Hence, we strived to develop and test the accuracy of a non-invasive optical tympanometry device to evaluate pediatric OM by detecting middle ear effusion (MEE). To achieve this, we first assessed the validity of the technology and its diagnostic algorithm via an *in vitro* bench-top model, which is the topic of this manuscript.

2. Methods

Institutional Review Board consideration was not applicable as this study was performed in an *in vitro* model in a laboratory setting. The bench-top model of the optical tympanometry device (Fig. 1A) used a broadband black body light source and spectrometer to obtain reflectance measurements within spectral frequencies of 450–1100 nm from the *in vitro* model of ear canal and tympanic membrane. Our prototype instrument utilized two compact waveguides housed within a commercially available speculum (Welch Allyn, NY, USA) currently used for clinical ear examination (Fig. 1B). One waveguide was coupled to a broadband light source (3100K, Ocean Optics, FL, USA) used for illumination and the second one was used to collect remitted light, which was then measured using a spectrometer system (USB2000, Ocean Optics, FL, USA). Two 750 μm glass fibers were spread approximately 4 mm center on center, 10 mm apart from the *in vitro* model’s surface

and used for illumination and data collection, respectively (Fig. 1). The bench-top model was held stationary and the *in vitro* model was moved and replaced before each measurement resulting in 30 seconds interval between each measurement.

The *in vitro* model of the ear simulated the physiological attributes of a patient with MEE or a healthy ear (Fig. 2). The model included 3 distinct regions: the ear canal/cerumen zone, the tympanic membrane/erythema zone, and the fluid zone. The tympanic membrane and middle ear were modeled by stretching a collagen-rich porcine submucosa (commercially available off the shelf) over the opening of a 10 mL amber glass vial. Erythema was simulated using fresh whole blood placed between glass cover slips, which could be placed directly onto the porcine submucosa. The two pressed glass slides with fresh whole blood in between created one layer of blood cells, modeling tympanic membrane's capillary flow in the case of acute OM. The canal/cerumen zone was simulated by placing human cerumen between a second set of glass cover slips, which could be then placed either on top of the erythema layer, or directly onto the submucosa, depending on which of the following clinical situations we were modeling. a) In purulent MEE representing acute OM, the tympanic membrane and middle ear exhibit erythema and the middle ear fills with a cloudy fluid (effusion). The cloudy fluid was modeled by filling the glass vial with a highly scattering 10% (v/v) whole milk solution. This turbid fluid (whole milk) representing middle ear effusion, in addition to the mentioned pressed fresh whole blood representing erythema, were the main two signatures of acute OM in our setting. b) In serous MEE representing serous OM, the middle ear fills with a non-cloudy fluid, modeled with water. c) Healthy ears do not exhibit erythema or fluid in the middle ear cavity (air filled glass vial).

Each of the three models was assessed with or without the cerumen simulation to assess its potential confounding effect and whether it was a barrier to correct detection. The colorless glass cover slips were 0.10–0.21 mm thick and had a negligible effect on the reflectance spectra. Figure 3 depicts absorption spectra of oxygenated hemoglobin (HbO2), deoxygenated hemoglobin (rHb), water (37 °C), and fat.[9–11] It was expected that the overall optical attenuation in our model system would approximate the superposition of the known spectra of HbO2, rHb, water, and fat (cerumen). To assess whether these spectral differences can comprise a discrete wavelength measurement capable of distinguishing between different *in vitro* modeled ear states, we aimed to build two logistic classifiers using MATLAB R2010b (The MathWorks Inc.). In our case, the logistic classifier was a linear and binary classification model with the goal of maximizing the classification accuracy based on attenuations at particular wavelengths. The net effect was to create a separating hyperplane in a parameter space defined by the attenuation profile of all used wavelengths.[12] To correctly classify all *in vitro* middle ear states, first classifier would classify purulent effusion against all other conditions and the second would classify serous effusion against the rest of conditions. As such, each classifier would employ wavelength hypothesized to correlate with erythema (e.g., HbO2 peak at 540 nm and rHb peak at 560 nm in Fig. 3), cerumen (e.g., significant attenuation due to fat at 500 nm in Fig. 3), and fluid/air (e.g., water peak at 975 nm in Fig.3). It was expected that the optical reflectance of each condition would comprise a combination of the known absorptions of HbO2, rHb, cerumen (fat), and water, plus a baseline at each wavelength related to our particular model system.

3. Results

We collected data from 60 samples including 10 repeats of 6 different combinations corresponding to ear conditions [3 types of vial fillings (milk, water, and air) × 2 cerumen states (with and without ear cerumen)]. Figure 4 shows the log inverse reflectance of six model conditions: normal healthy ear, serous MEE, and purulent MEE with and without cerumen. The healthy ear (Figure 4A) was considered as a baseline upon which absorption contrasts related to hemoglobin, cerumen, and water could be compared. The increased attenuation and decreased slope between 400–600 nm in panels B, D, and F is related to the presence of cerumen. The water attenuation at 970 nm is observed in serous simulations with and without cerumen (Figures 4C & D), and in both purulent simulations (Figures 4E & F). The HbO2 peak at 540 nm and rHb peak at 560 nm are clearly visible in panels E and F.

Two logistic classifiers were successfully developed for distinguishing different modeled ear states. The first classifier detected purulent MEE (with or without cerumen) against all other conditions (Figure 5A) and the second classifier detected serous MEE (with or without cerumen) against the rest of conditions (Figure 5B). Together, these models enabled logic (Figure 5C) that correctly classified all *in vitro* middle ear states. We employed reflectance values at 500 nm (significant cerumen attenuation), 540 nm (HbO2), 560 nm (rHb), 577 nm (HbO2), 750 nm and 930 nm (reference values), and 975 nm (water peak). Importantly, because the logistic classifier operates on the log inverse reflectance values, including reference values at 750 nm and 930 nm offer a means of fitting the baseline attenuation which is related to the model system and the presence or absence of cerumen to enhance the contrast of attenuation related to water and hemoglobin. Both models achieved 100% accuracy as assessed by leave-one-out and k-fold cross validation which provide accurate metrics that are less sensitive to the peculiarities of this particular dataset.

4. Discussion

We assessed the optical and spectroscopic properties of the *in vitro* model of the middle ear space for potential non-invasive, rapid, and objective evaluation of middle ear effusion. By interchanging fluid types and glass cover slips, we made measurements on combinations corresponding to different ear pathologies (e.g., blood over milk solution, and cerumen representing acute OM). We demonstrated that our algorithmic approach is capable of separating simulated serous and purulent effusions from those corresponding to healthy ears (i.e., air filled vial). This is a crucial step in developing an otoscope-like device that collects full spectrum data from patients' ears in order to accurately recognize middle ear effusion and potentially acute OM.

The diagnosis of acute OM is often subjective and inaccurate. In practice, it is typical for a febrile child with an earache who presents with an erythematous tympanic membrane on otoscopic examination to be prescribed antibiotics. Despite updated clinical guidelines dating to 1994, no significant reduction in unnecessary antibiotic prescription rates has been achieved.[8] This calls for an improved and objective methods to easily and reliably diagnose OM, such as the assessment of the potential presence of middle ear effusion via its

optometric characteristics. Current clinical practice guidelines recommend use of pneumatic otoscopy or acoustic tympanometry as an accurate means of assessing the presence or absence of middle ear effusion.[8,13] Key action statement 1C of AAP guideline for acute OM recommends that “clinician should not diagnose acute otitis media in children who do not have middle ear effusion (based on pneumatic otoscopy and/or tympanometry)”.

Pneumatic otoscopy requires seal of the ear canal and good visualization of the tympanic membrane while the patient is not moving. Unfortunately, only a minority of primary care physicians routinely utilize pneumatic otoscopy to diagnose OM, likely due to unavailability, discomfort to patient, or poor technique causing an unreliable response. Acoustic tympanometry is also recommended by AAP and AAO-HNSF, which also relies on sealing the ear canal to measure sound reflectance, as an adjunctive option to pneumatic otoscopy.[5,8,13] However, this procedure can be uncomfortable and requires an air-tight seal on the ear for about 10–20s, which is difficult to achieve in an uncooperative young patient. As a result, acoustic tympanometry is also not commonly practiced in primary care where most patients with suspected otitis media are seen.[1–3,8] The majority of emerging technologies for diagnosis of OM are not widely accepted due to their lack of proven superiority compared to otoscopy.[14] In standard practice, clinicians typically rely on visual cues only, e.g. redness, which widely lacks specificity and positive predictive value.[15] The high accuracy achieved in our *in vitro* system leads us to hypothesize that it might be possible to identify MEE through cerumen *in vivo*.

New technologies are continuously evolving for middle ear imaging and characterizations.[14,16–18] These non-invasive technologies can potentially translate to hand-held otoscope devices to provide tympanic membrane information such as extent of retraction and perforation margin as well as detecting any effusion, purulence, or biofilms behind the tympanic membrane.[19,20] Diffuse optical spectroscopy (DOS) is one technology which has been utilized for evaluating different biological tissues and diagnosis of several pathologies.[21–26] This method provides quantitative and functional information based on optical absorption and scattering properties that cannot be obtained with other imaging methods. DOS-measured absorption spectra are used to determine the tissue concentrations of oxyhemoglobin (HbO2), deoxyhemoglobin (rHb), lipid, and water, as well as to provide an index of tissue hemoglobin oxygen saturation. Tissue-scattering spectra provide insight into epithelial, collagen, and lipid contributions of target of interest (i.e., tympanic membrane and middle ear). The application of spectroscopy and fluorescence spectroscopy to assist detection of OM is not new. In the mid 1990s, Sorrell *et al.* identified spectroscopic profiles of common OM pathogens,[27] which paved the way for Zhao *et al.*’s recent success in combining Raman scattering spectroscopy and low coherence interferometry in better characterizing microbial pathogens.[28] Previous studies using spectroscopy to detect MEE have ignored the confounding effects of cerumen. This experiment builds on the previous knowledge by demonstrating that it is possible to overcome this confounding to spectroscopic detection of MEE *in vitro*. Future work will build on these results and test the hypothesis that the confounding effects of cerumen can be mitigated *in vivo*.

A relatively recent method for evaluating the middle ear is a non-invasive medical imaging technology referred to as optical coherence topography (OCT). OCT has been utilized by

Monroy *et al.*,[16,18] Shelton *et al.*,[29] and Nguyen *et al.*[30] to detect presence of middle ear biofilm and evaluate tympanic membrane thickness. Likewise, Wong *et al.* and Pande *et al.* have benefited from similar imaging technologies to analyze changes in tympanic membrane dynamics/position and middle ear pressure to subsequently characterize OM.[31,32] More recently, a device which utilizes ultrasound signal processors and excitation generators to detect fluid type (no fluid, serous fluid, purulent fluid) behind the tympanic membrane and thus characterize MEE has entered the market.[33] Continues advancement in the field of detecting MEE is crucial, since incorrect diagnosis of OM can lead to unnecessary antibiotic prescription, preventable adverse affects, microorganism resistance, and a high cost burden to the healthcare system.[34,35]

Sundberg *et al.* and later Schmilovitch *et al.* have utilized DOS for diagnosis of acute OM; however, they both did not account for the presence of cerumen.[25,26] Also, our utilization of discrete wavelength profiles can lead to achieving similar diagnostic accuracy with less expensive device designs in the future (e.g., using LED emitters) which will be valuable for smaller clinic settings and independent providers. Cerumen is typically thick as compared to the tympanic membrane, highly light scattering, and could limit the applicability of their technologies in primary care practice. We developed a novel algorithm using DOS technology specifically designed to work through cerumen for the diagnosis of middle ear effusion. The model system provided a controlled means of assessing the feasibility of a spectroscopic approach to assess serous and purulent effusions in the presence or absence of cerumen. In our study, optical attenuation related to hemoglobin and water provided a means of discriminating serous and purulent effusions from normal when cerumen is present. This work, considered as a necessary first step, will be followed by an *in vivo* experiment to evaluate feasibility and efficacy in patients. In subsequent experiments, results from Monroy *et al.* and Pande *et al.* characterizing thickness distributions for *in vivo* tympanic membrane models can further optimize our degree and intensity of light penetration for an ideal diagnostic sensitivity and specificity.[16,32] Furthermore, our *in vitro* bench-top model's approximate time of diagnosis which was similar across possible differentials was less than ten seconds, which will translate to a convenient and efficient *in vivo* hand-heled device in the future. Future *in vivo* studies aimed at collecting data from children undergoing myringotomy and tube placement are warranted to further elucidate the validity and efficacy of our optical tympanometry device in diagnosing acute OM by detecting middle ear effusion.

5. Conclusion

This proof-of-concept *in vitro* study addressed an unmet need by introducing a device that easily and accurately can assess middle ear effusion. This bench-top study will enable us to refine our approach and give us the confidence we can achieve success in the clinical setting with our prototype spectrometer system. It is possible that in the near future, non-invasive optical ranging techniques will transform from diagnostic tools into screening assessments at primary care offices.[24]

Acknowledgements

Mehdi Abouzari, MD, PhD; is supported by the National Center for Research Resources and the National Center for Advancing Translational Sciences, National Institutes of Health, through Grant TL1TR001415-05. The content is solely the responsibility of the authors and does not necessarily represent the official views of the NIH.

References

1. Miser WF. To treat or not to treat otitis media--that's just one of the questions. J Am Board Fam Pract 2001; 14: 474–476. [PubMed: 11757893]
2. Monasta L, Ronfani L, Marchetti F, et al. Burden of disease caused by otitis media: systematic review and global estimates. PLoS One 2012; 7: e36226. [PubMed: 22558393]
3. Kaur R, Morris M, Pichichero ME. Epidemiology of acute otitis media in the postpneumococcal conjugate vaccine era. Pediatrics 2017; 140: e 20170181.
4. National Hospital Ambulatory Medical Care Survey: 2015 Emergency Department Summary Tables. Centers for Disease Control and Prevention, 2015.
5. Rosenfeld RM, Shin JJ, Schwartz SR, et al. Clinical practice guideline: otitis media with effusion (update). Otolaryngol Head Neck Surg 2016; 154: S1–S41. [PubMed: 26832942]
6. American Academy of Pediatrics Subcommittee on Management of Acute Otitis Media. Diagnosis and management of acute otitis media. Pediatrics 2004; 113: 1451–1465. [PubMed: 15121972]
7. Pichichero ME. Acute otitis media: Part I. Improving diagnostic accuracy. Am Fam Physician 2000; 61: 2051–2056. [PubMed: 10779248]
8. Lieberthal AS, Carroll AE, Chonmaitree T, et al. The diagnosis and management of acute otitis media. Pediatrics 2013; 131: e964–e999. [PubMed: 23439909]
9. Hale GM, Querry MR. Optical Constants of Water in the 200-nm to 200-microm Wavelength Region. Appl Opt 1973; 12: 555–563. [PubMed: 20125343]
10. Takatani S, Graham MD. Theoretical analysis of diffuse reflectance from a two-layer tissue model. IEEE Trans Biomed Eng 1979; 26: 656–664. [PubMed: 544437]
11. van Veen RL, Sterenborg HJ, Pifferi A, et al. Determination of visible near-IR absorption coefficients of mammalian fat using time- and spatially resolved diffuse reflectance and transmission spectroscopy. J Biomed Opt 2005; 10: 054004. [PubMed: 16292964]
12. Zhang Y, Wang Q, Li B, et al. Changes in Attenuated Total Reflection Fourier Transform Infrared Spectra as Blood Dries Out. J Forensic Sci 2017; 62: 761–767. [PubMed: 27982433]
13. Harmes KM, Blackwood RA, Burrows HL, et al. Otitis media: diagnosis and treatment. Am Fam Physician 2013; 88: 435–440. [PubMed: 24134083]
14. Marom T, Kraus O, Habashi N, Tamir SO. Emerging Technologies for the Diagnosis of Otitis Media. Otolaryngol Head Neck Surg 2019; 160: 447–456. [PubMed: 30396324]
15. Bhetwal N, McConaghy JR. The evaluation and treatment of children with acute otitis media. Prim Care 2007; 34: 59–70. [PubMed: 17481985]
16. Monroy GL, Shelton RL, Nolan RM, et al. Noninvasive depth-resolved optical measurements of the tympanic membrane and middle ear for differentiating otitis media. Laryngoscope 2015; 125: E276–E282. [PubMed: 25599652]
17. Monroy GL, Pande P, Nolan RM, et al. Noninvasive in vivo optical coherence tomography tracking of chronic otitis media in pediatric subjects after surgical intervention. J Biomed Opt 2017; 22: 1–11.
18. Monroy GL, Hong W, Khampang P, et al. Direct analysis of pathogenic structures affixed to the tympanic membrane during chronic otitis media. Otolaryngol Head Neck Surg 2018; 159: 117–126. [PubMed: 29587128]
19. Park K, Cho NH, Jeon M, et al. Optical assessment of the in vivo tympanic membrane status using a handheld optical coherence tomography-based otoscope. Acta Otolaryngol 2018; 138: 367–374. [PubMed: 29125012]
20. Shelton RL, Nolan RM, Monroy GL, et al. Quantitative pneumatic otoscopy using a light-based ranging technique. J Assoc Res Otolaryngol 2017; 18: 555–568. [PubMed: 28653118]

21. Shah N, Cerussi AE, Jakubowski D, et al. The role of diffuse optical spectroscopy in the clinical management of breast cancer. Dis Markers 2003–2004; 19: 95–105.
22. Nakamiya N, Ueda S, Shigekawa T, et al. Clinicopathological and prognostic impact of imaging of breast cancer angiogenesis and hypoxia using diffuse optical spectroscopy. Cancer Sci 2014; 105: 833–839. [PubMed: 24766271]
23. Lee CW, Cooper RJ, Austin T. Diffuse optical tomography to investigate the newborn brain. Pediatr Res 2017; 82: 376–386. [PubMed: 28419082]
24. Wan QS, Wang T, Zhang KH. Biomedical optical spectroscopy for the early diagnosis of gastrointestinal neoplasms. Tumour Biol 2017; 39: 1010428317717984. [PubMed: 28671054]
25. Sundberg M, Borga M, Knutsson H, et al. Fibre-optic array for curvature assessment: application in otitis diagnosis. Med Biol Eng Comput 2004; 42: 245–252. [PubMed: 15125156]
26. Schmilovitch Z, Alchanatis V, Shachar M, Holdstein Y. Spectrophotometric otoscope: a new tool in the diagnosis of otitis media. J Near Infrared Spectrosc 2007; 15: 209–215.
27. Sorrell MJ, Tribble J, Reinisch L, Werkhaven JA, Ossoff RH. Bacteria identification of otitis media with fluorescence spectroscopy. Lasers Surg Med 1994; 14: 155–163. [PubMed: 8183049]
28. Zhao Y, Monroy GL, You S, et al. Rapid diagnosis and differentiation of microbial pathogens in otitis media with a combined Raman spectroscopy and low-coherence interferometry probe: toward in vivo implementation. J Biomed Opt 2016; 21: 107005. [PubMed: 27802456]
29. Shelton RL, Jung W, Sayegh SI, et al. Optical coherence tomography for advanced screening in the primary care office. J Biophotonics 2014; 7: 525–533. [PubMed: 23606343]
30. Nguyen CT, Jung W, Kim J, et al. Noninvasive in vivo optical detection of biofilm in the human middle ear. Proc Natl Acad Sci U S A 2012; 109: 9529–9534. [PubMed: 22645342]
31. Won J, Monroy GL, Huang PC, et al. Quantitative Pneumatic Otoscopy Using a Light-Based Ranging Technique. J Assoc Res Otolaryngol 2017; 18: 555–568. [PubMed: 28653118]
32. Pande P, Shelton RL, Monroy GL, Nolan RM, Boppart SA. Low-cost hand-held probe for depth-resolved low-coherence interferometry. Biomed Opt Express 2016; 8: 338–348. [PubMed: 28101422]
33. Moehring M, Chesavage J, Singh R, et al. Apparatus and method for characterization of acute otitis media. https://patents.google.com/patent/WO2017011035A1/en
34. Dagan R, Leibovitz E, Leiberman A, Yagupsky P. Clinical significance of antibiotic resistance in acute otitis media and implication of antibiotic treatment on carriage and spread of resistant organisms. Pediatr Infect Dis J 2000; 19: S57–S65. [PubMed: 10821473]
35. Cunha BA. Antibiotic side effects. Med Clin North Am 2001; 85: 149–185. [PubMed: 11190350]

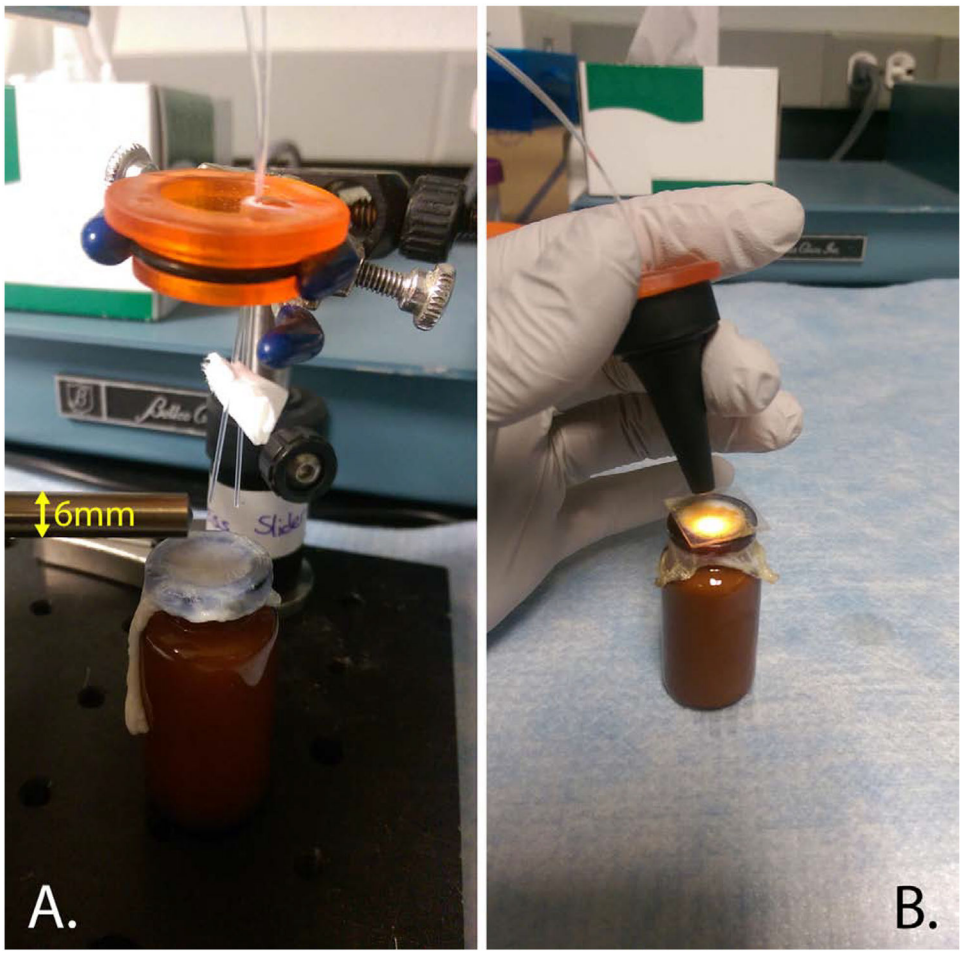

Figure 1.

(A) The bench-top model of the optical tympanometry device with 6 mm drill bit held in place for scale. (B) The prototype instrument utilized two waveguides housed within a Welch Allyn speculum for illumination and collecting remitted light.

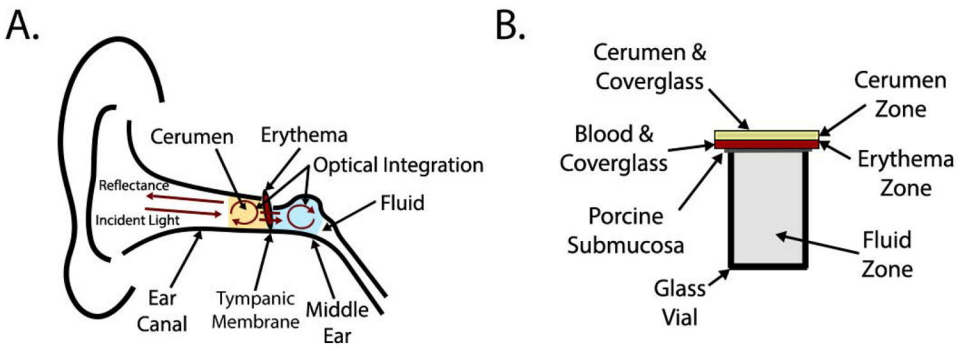

Figure 2.

(A) Depicted figure of middle ear effusion (MEE); cerumen in the ear canal lateral to the tympanic membrane, an erythematous tympanic membrane, and middle ear filled with turbid fluid. (B) *In vitro* model of MEE with cerumen.

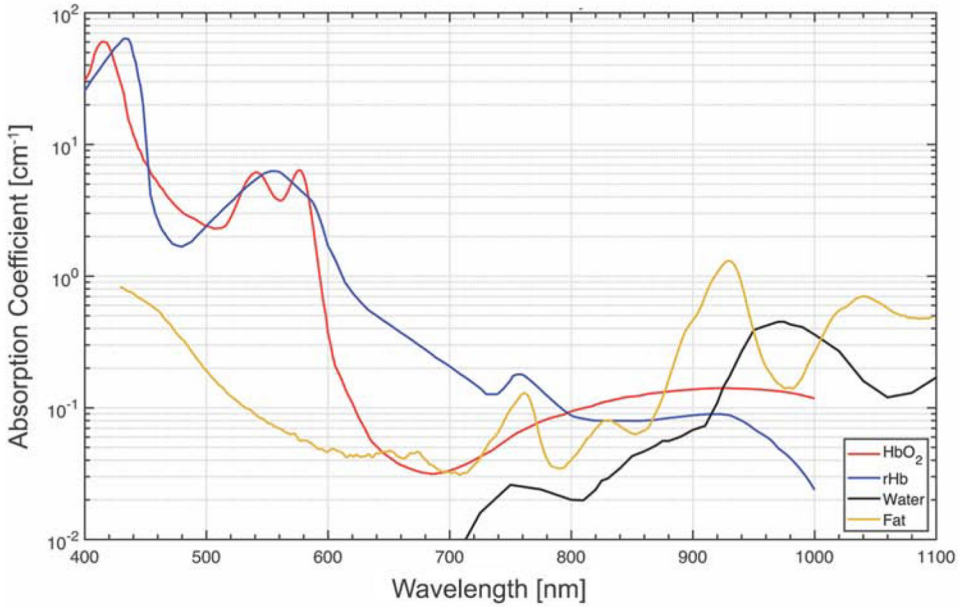

Figure 3.

Absorption coefficient spectra of oxygenated hemoglobin (HbO2), deoxygenated hemoglobin (rHb), water, and fat (cerumen). These components are expected to provide the primary absorption contrasts in MEE models.

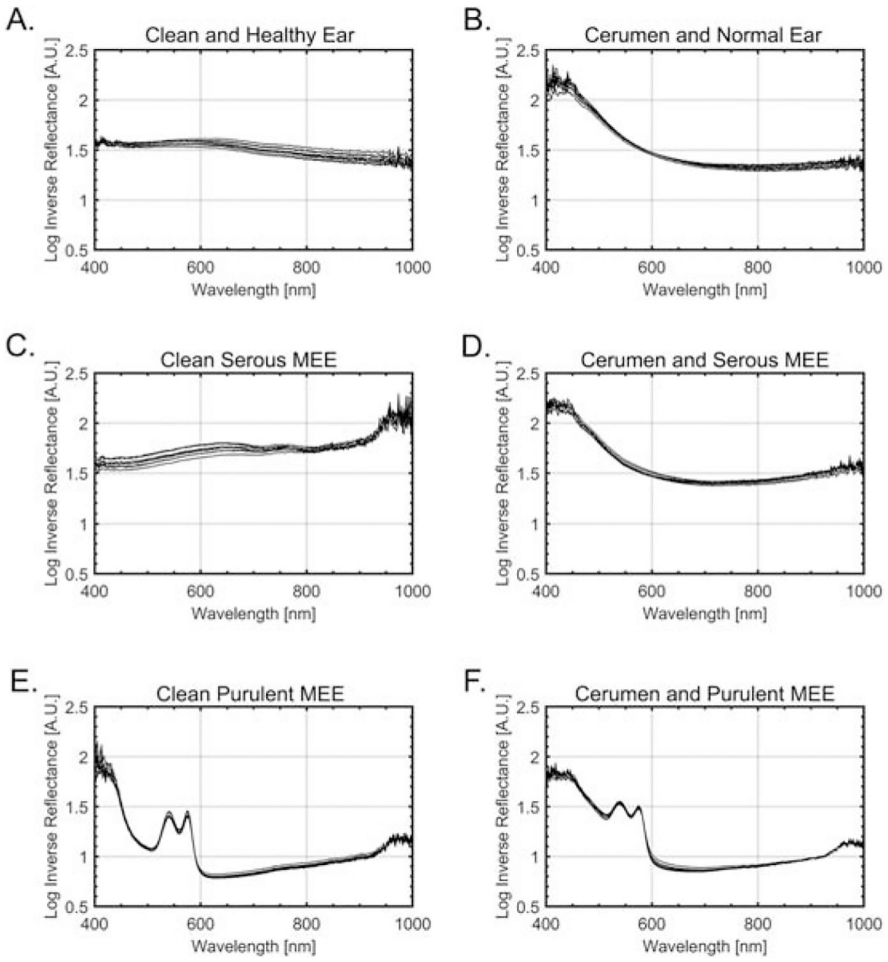

Figure 4.

Three different simulations with 10 repeats each corresponding to different middle ear states with (right) and without (left) cerumen. Each simulated condition has a distinct spectral profile, which was then employed by our algorithm to discriminate clean and cerumen-covered purulent and serous MEE.

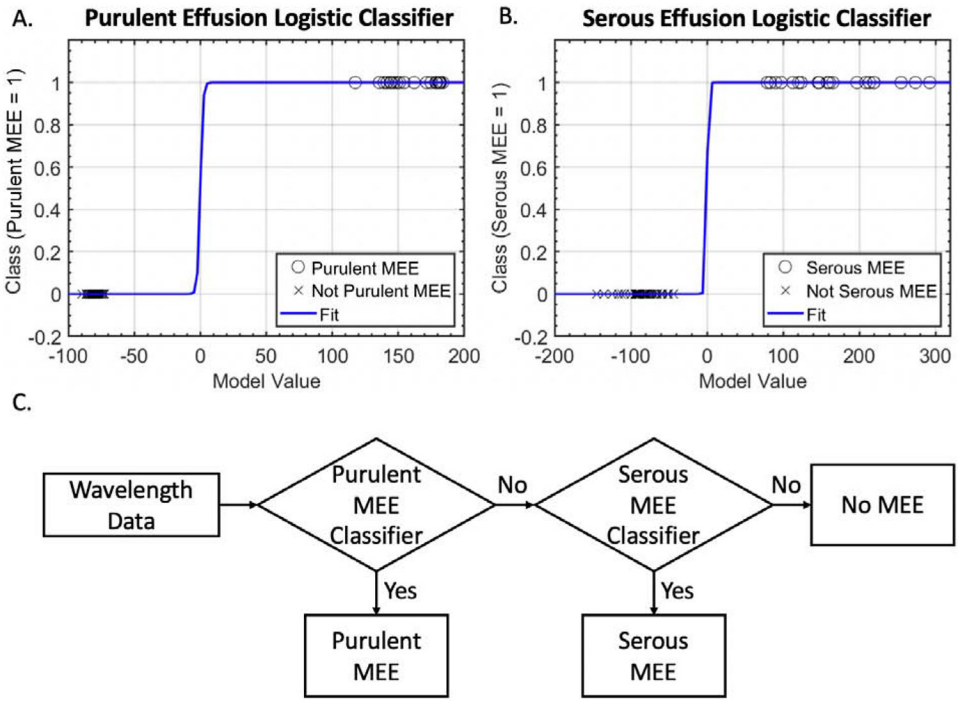

Figure 5.

MEE classification. (A) Purulent effusion logistic classifier with X-axis corresponds to the weighted sum of aborption coefficient spectra and Y-axis shows the output of the logistic model. Zero corresponds to no mucoid MEE and 1 corresponds to mucoid MEE. (B) Serous effusion logistic classifier with X-axis corresponds to the weighted sum of aborption coefficient spectra and Y-axis shows the output of the logistic model. Zero corresponds to no serous MEE and 1 corresponds to serous MEE. (C) Flow chart of logic employing purulent and serous MEE classifiers that enables correct classification of all simulated *in vitro* middle ear states.